Precision Doping of Polyelectrolyte Complexes: Insight on the Role of Ions

Mo Yang, Zachary Digby, Joseph B. Schlenoff*

Department of Chemistry and Biochemistry

The Florida State University, Tallahassee, FL 32306

Abstract

The properties of polyelectrolyte complexes and coacervates, both termed PECs, are influenced strongly by their ion and water content. Water plasticizes PECs, reducing their modulus and glass transition temperature, T_g . In this work, a hydrated PEC with a T_g near room temperature, made from poly(diallyldimethylammonium), PDADMA, and poly(styrene sulfonate), PSS, was precisely doped with $^{22}\text{Na-labeled}$ sodium salts along a Hofmeister series. A distinctive change in the rate of doping *versus* added salt concentration was observed for all salts. This transition was interpreted to reflect a change in ion-accessible volume coinciding with a change in the role of added salt from counterions for the polyelectrolytes, paired directly and within one water molecule of the charge on the polymer backbone, to a mix of counterions and co-ions, which do not have a specific location within the PEC. Isothermal calorimety for PEC made in, and doped by, NaCl showed two clear regions for enthaply change, ΔH , before and after the doping transition. The higher ΔH region was correlated with the counterion role, an indirect measure of the location of ions within the PEC.

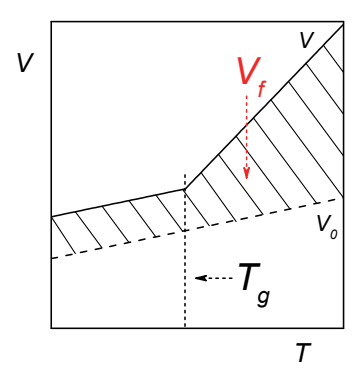
Introduction

When solutions of oppositely-charged macromolecules are mixed, an amorphous complex of the two polymeric components may spontaneously form.^{1, 2, 3, 4, 5} This phenomenon was first studied systematically for biopolymers or their derivatives, which are generally fluid-like and were termed coacervates.⁶ When synthetic polyelectrolytes, having higher net charge densities, were first complexed they were noted to have a more solid morphology.⁷ Coacervates and complexes from polyelectrolytes, both termed PECs, occupy different ends of a continuum of viscoelastic response that is determined by the water content, salt concentration, stoichiometry, molecular weight and polymer composition.⁸ For example, an early observation² concerned the dramatic difference in mechanical properties for hydrated *versus* dry PECs (rubbery *versus* brittle) indicating a strong plasticizing effect of water.

In addition to softening PECs, water brings down the glass transition from unmeasurably high for dry materials 9 (greater than the thermal stablity of the material) to within laboratory measurement range. $^{10, \, 11}$ When in contact with aqueous solution, the equilibrium water content of PECs is in the range 30-70 wt%, 12 substantially greater than engineering polymers but also much less than a hydrogel. The specific combination of poly(diallyldimethylammonium), PDADMA, and poly(styrene sulfonate), PSS, equilibrated with water was observed to have a glass transition temperature, T_g , just above room temperature. $^{13, \, 14, \, 15, \, 16}$

The addition of salt introduces more water (typically) into the PEC and also breaks pairs between polycation, Pol⁺, and polyanion, Pol⁻, repeat units, reducing the instantaneous physical crosslinking density.¹⁷ The combined effects of water and salt in decreasing the modulus and viscosity of PECs, a property known as "saloplasticity" (actually hydrosaloplasticity),¹⁸ enables the processing by extrusion,¹⁹ embossing,^{20, 21} spin coating,²² bar coating,²³ pressure molding²⁴ etc. of an otherwise "unprocessible" material.

A hydrated PEC may be considered to be a heavily plasticized, physically crosslinked amorphous polymer blend. There are several interesting aspects concerning such a material, where the mechanical properties and T_g are strong functions of water content. From a classical perspective, water, as with any plasticizer, introduces free volume for polymer chains to access. When dry, in addition to a high modulus, PDADMA/PSS was measured to have quite a high density (1.27 g cm $^{-3}$), extremely low permeability to gases, 27 and could not be swelled by solvents with a molecular volume greater than about 50 Å 3 . These observations are consistent with a low free volume for the dry state. Free volume added by a plasticizer such as water lowers the temperature for the transition to the rubbery state, illustrated by Scheme 1, which presents an accepted view of this subtle change in volume versus temperature at T_g . 29



Scheme 1. Change in polymer volume *versus* temperature at the glass transition. The total volume, V, which increases with temperature, includes the free volume (V_f , shaded) and the polymer molecular volume, V_o . At the glass transition, T_g , there is a change in the slope as additional free volume accumulates.

The glass transition in general is intriguing because few microscopic structural changes can be observed while the macroscopic mechanical properties change substantially. $^{30, 31}$ Recent quantitative efforts have linked T_g in PECs to water content. For example, Zhang et al., 10 showed that T_g decreased as a function of the water hydrating Pol+Pol- pairs, also known as intrinsic sites, consistent with plasticizer behavior. Some aspects of T_g in PECs are nontraditional. For example, the modulus on the "glassy" side of T_g is rather low, a few MPa, rather than the GPa range usually seen in engineering polymers. This property, a result of the high water content, means the change in modulus as PECs pass through the T_g is not as marked as it would be for classical unplasticized polymers.

Doping is a generic term for introducing salt, MA (M⁺ cation, A⁻ anion), into hydrated PECs by increasing the concentration of MA in the solution, [MA]_s, in which the complexed Pol⁺Pol⁻, is immersed

$$rMA_s + Pol^+Pol^- \rightarrow Pol^+Pol^-(MA)_r$$
 [1]

where r is the mole ratio, or doping level, of salt to polyelectrolyte in any form within the PEC, termed PE^{32}

$$r = \frac{[MA]_{PEC}}{[PE]_{PEC}}$$
 [2]

 T_g for the PDADMA/PSS system doped with NaCl exhibited ¹⁵ a time-temperature-salt doping equivalence (superposition) ^{33, 34, 35, 36, 37}

$$T_g = 38 + 2.3 \ln f - 20[NaCl]^{6/5}$$
 [3]

where f is the frequency of the mechanical perturbation. In other words, salt doping decreased the T_g in a systematic way. In the present work, PDADMA/PSS PEC was doped with a high level of precision using radiolabeled sodium salts using anions along a Hofmeister series. Precision doping measurements revealed a new feature consistent with a change in free volume at T_g . This feature is believed to be unique to solid-like PECs. The role of MA within the PEC was assigned to that of counterions, which break Pol*Pol* pairs, and co-ions, which simply occupy some of the accessible volume introduced by doping. This work also attempted to establish whether the T_g decrease is attributable to water introduced by doping and/or to breaking Pol*Pol*physical crosslinks.

Experimental

Materials. PDADMA(CI) (Ondeo-Nalco, molar mass ca. 400,000 g mol⁻¹) and PSSNa (AkzoNobel, VERSA TL 130, molar mass ca. 200,000 g mol⁻¹), for preparing extruded PECs, were used as received. Sodium acetate (Sigma-Aldrich), sodium chloride (Sigma-Aldrich), sodium bromide (Sigma-Aldrich), sodium iodide (Sigma-Aldrich) and sodium perchlorate (Sigma-Aldrich) were dried under vac for 24 h. Deionized water (18 MΩ cm Barnstead, E-pure) was used to prepare salt solutions. 22 Na⁺-labeled NaCl (half-life 950 d, E_{max} = 511 keV, γ) was supplied by PerkinElmer with a specific activity of 914 Ci g⁻¹. PSS/PDADMA PEC tapes with a width of 2 cm and thickness about 1 mm were extruded from stoichiometric complex using a published procedure. ¹⁹ Complexation has the added benefit that nonpolymeric impurities are washed out during precipitation. PECs tablets with a thickness of ~1 mm and diameter of 8 mm for radiolabeling and rheology were cut from the tapes using a brass cork borer.

Radiolabeling. Radiolabeling experiments were performed to determine the doping behavior, or the salt content, of PSS/PDADMA PEC tablets exposed to salt solutions along a Hofmeister series: (NaAc, Ac = acetate, NaCl, NaBr, Nal and NaClO₄). For each salt, a series of 10.0 g "hot" 22NaA (A: anion) solutions with a range of salt concentrations was prepared with a specific activity of 5 × 10⁻⁴ Ci mol⁻¹. Molalities, m, used because of the convenience and precision of weighing, were converted to molarities. M. using standard conversion tables. Before radio-labeling experiments. PSS/PDADMA tablets were soaked in 0.1 m non-labeled NaCl for 24 h. For each salt (e.g. NaBr), the tablet was first placed in 10 g of the lowest concentration "hot" solution (e.g. 0.1 m ²²NaBr). After doping, the wet tablet was quickly dabbed dry and weighed. The tablet was then placed on top of a plastic scintillator (SCSN-81, Kuraray, 3 mm thickness, 38 mm diameter) which was in good optical contact with an RCA 8850 photomultiplier tube (PMT) powered at -2300 V. The PMT was connected to a frequency counter (Philips PM6654C) with 10 s gate time and -20 mV pulse threshold. The tablet was counted for at least 15 mins. A time vs. count rate plot was obtained to determine when the ion content of the tablet reached equilibrium, indicated by a plateau in count rate. After counting, the tablet was soaked in the "hot" solution with a higher concentration (e.g. 0.2 m ²²NaBr) and the same equilibration and counting steps repeated. To convert counts to moles of salt, calibration curves were collected by placing aliquots of the ²²Na⁺-labeled 1.0 m solution on top of the plastic scintillator. An undoped PSS/PDADMA tablet was used to cover the aliquots (see Supporting Information Figure S1 for calibration curves). Finally, tablets were rinsed in water for at least 24 h to remove salt, dried at 120 °C under vac for 24 h and weighed to obtain the mass of the polyelectrolytes only. The total counts accumulated for each sample ranged from 10000 to 50000 with respective counting errors of 1% and 0.4%. The background count rate was about 8 cps.

Rheology. A stress-controlled DHR-3 rheometer (TA Instruments) with 8 mm parallel plate geometry was used to measure the linear viscoelastic response of fully hydrated PECs. PSS/PDADMA tablets were first placed in the center of a custom-designed brass solvent reservoir. A compressive axial force of 1 N was applied to the tablet to prevent sample slip. The desired salt solution (unlabeled) was then transferred into the reservoir. A brass cap was placed on top of the reservoir to prevent water evaporation. Temperature ramp experiments were performed to obtain T_g of PSS/PDADMA tablets in salt solutions at 0.1 Hz with a ramp rate of 1 °C min⁻¹ and a strain of 0.01 %. An initial heat/cool cycle was performed to anneal samples before data collection. Frequency sweeps were performed from 0.01 to 100 Hz with a strain of 0.01 % at 15 °C above T_g . Amplitude sweep experiments were carried out to make sure the selected strain was within the linear viscoelastic regime.

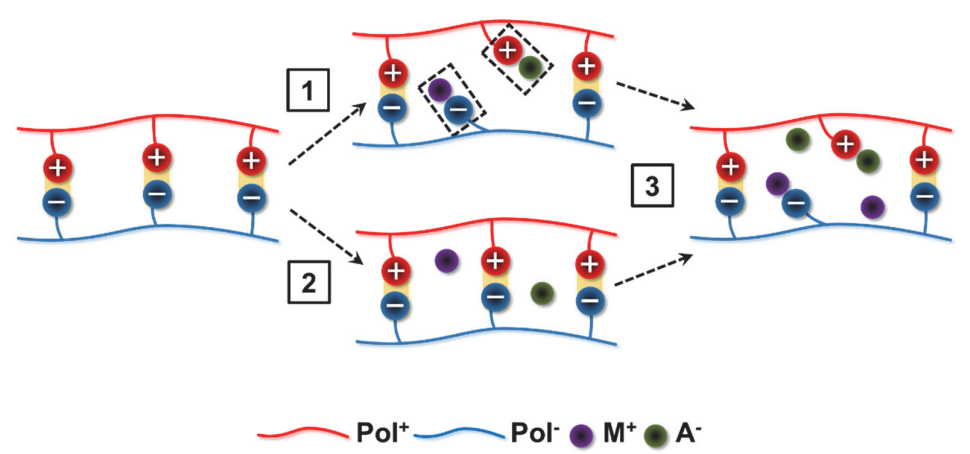
Isothermal Calorimetry. Poly(4-styrenesulfonic acid), (PSSH, molar mass = 75,000 g mol⁻¹, Sigma-Aldrich) was neutralized with NaOH to give PSSNa. PDADMA(Cl) (molar mass ca. 400,000) was from Sigma-Aldrich. Polyelectrolytes were dialyzed against deionized water for 3 days, with water replacement every 24 h. Solutions were then freeze dried (Labconco, FreeZone -105), then dried at 120 °C for 4 h, then moved immediately into an Ar-filled glove box equipped with an analytical balance. NaCl, NaI, and NaOCl₄ used in the solutions were dried in a similar manner and weighed in the glovebox. Solutions of PSSNa (10 mM, all polymer solution concentrations were based on the repeat unit) and PDADMA(Cl) (0.5 mM) were made with varying NaCl concentrations (0.1 – 0.9 M). Solutions of 10 mM PDADMA(Cl) with no salt and 0.1 M NaOCl₄ were prepared as well.

ITC was performed using a VP-ITC (MicroCal Inc.) instrument. The ITC instrument was calibrated with the internal y-axis calibration command followed by a standard titration between hydrochloric acid and Tris base. Prior to each ITC experiment, both the syringe solution and the sample cell solution were degassed for 10 min at room temp. Approximately 300 µL of 10 mM PSSNa in a precise [NaCl] was loaded into the syringe. 10 μL was manually discharged from the syringe to relieve any back pressure from purging and refilling the syringe. The sample cell (1.4138 mL) was washed and refilled with 0.5 mM PDADMA(CI) with an identical NaCl concentration. The syringe was then rotated at 260 rpm in the sample cell and 4 μL aliquots were injected into the sample cell at a rate of 0.50 μ L s⁻¹, with 240 s between injections. The heat flow was recorded as a function of time at 25.0 °C. These procedures were repeated for all NaCl concentrations. Enthalpies were calculated by summing the total heat generated to the end point with a small correction for the background, which was obtained from points following the end point. The dilution of the syringe solution was accounted for in the final enthalpy values. The interaction energy of PDADMA+ with I- or ClO₄- was measured by injecting 10 mM PDADMA(CI) into 0.10 M solutions of NaI or NaClO₄. Enthalpies of exchange/precipitation were obtained by summing the total heat generated over 30 injections.

Results and Discussion

Doping: Breaking Pairs versus Filling Space.

To an initial approximation, doping breaks pairs between oppositely-charged polyelectrolytes Pol⁺ and Pol⁻, illustrated in Scheme 2, Path 1.



Scheme 2. Possible locations for counterions entering a PEC. An ion-free, intrinsic PEC is shown on the left. Salt ions M⁺ and A⁻ dope the PEC, either breaking a Pol⁺Pol⁻

pair and acting as counterions (Path 1); or they do not formally break Pol⁺Pol⁻ pairs and remain co-ions (Path 2). Paths 1 and 2 can occur sequentially or simultaneously to give a mix of counter- and co-ions (shown on the right).

lons in Scheme 2, Path 1, are specifically paired with Pol⁺ and Pol⁻ and are thus termed *counterions*. Alternatively, ions enter the PEC and remain unassociated with Pol⁺ or Pol⁻, Path 2. These are termed *co-ions*. It is likely that both Paths are taken simultaneously or sequentially so that the PEC eventually contains a steady state mixture of counter- and co-ions, shown on the right in Scheme 2.

The overall salt content within a uniform PEC is established by a simple Donnan equilibrium, which balances the entropy (number density) of ions outside and inside the PEC phase. Specific interactions, often accompanied by a measurable rearrangement of water in a hydration shell, are signalled by changes in enthaply of PEC formation, ΔH_{PEC} . If ΔH_{PEC} is negative, the solution ion concentration, [MA]_s, in theory, exceeds the PEC ion concentration, [MA]_{PEC}. If ΔH_{PEC} is positive, [MA]_{PEC} > [MA]_s. Signal PEC ion concentration, [MA]_s.

Qualitatively, the amount of doping follows a Hofmeister series,^{40, 41} wherein hydrophobic MA ions are more efficient at doping. A "standard" Hofmeister series might include small univalent ions such as acetate, chloride, bromide, iodide, perchlorate (less to more hydrophobic). An "extended" Hofmeister series might also use organic ions to enhance the hydrophobic nature of the charge. For example, ions used in ionic liquids⁴² are often quite hydrophobic.

The efficiency of MA at breaking, or unpairing, Pol^+Pol^- pairs is given by a constant K_{unpair}

$$M_S^+ + A_S^- + Pol^+ Pol^- \to Pol^+ A_{PEC}^- + Pol^- M_{PEC}^+$$
 [4]

$$K_{unpair} = \frac{y^2 [PE]_{PEC}}{(1-y)[MA]_s^2}$$
 [5]

where y is the fraction of Pol⁺Pol⁻ pairs broken.³² The inverse of this describes the pairing equilibrium for PEC formation. Pol⁺Pol⁻ pairs and counterion-compensated repeat units are, respectively, known as "intrinsic" and "extrinsic" sites.

If y = 1, all Pol⁺Pol⁻ pairs are broken and the PEC may dissolve.⁴³ An older definition of the stability of PECs is termed the "salt resistance,"⁴⁴ which is the critical concentration of MA, [MA]_c, that must be added to dissolve the PEC. The exact point where PECs dissolve can be difficult to observe, and not all PECs dissolve, even if enough salt is added to reach y = 1 (for example, one of the polyelectrolytes might be insoluble in the salt).

The population of ions within the PEC, reprented by Scheme 2, may be broken down into a fraction f acting as counterions, and a fraction 1-f as coions. It is evident that y represents the counterion fraction, thus y = fr. Because r can greatly exceed 1, not all the ions that enter a PEC necessarily break Pol⁺Pol⁻ pairs, reflected in Scheme 2. In fact, for the PDADMA/PSS system doped with KBr, which is nearly athermal, $r \approx 5$ as y approaches 1.8 At this point f = 0.2, or there are 4 times as many co-ions as counterions in the PEC. This "salt inflation" of a stoichiometric PEC ([Pol⁺] = [Pol⁻]) close to y = 1 is a consequence of the Donnan equilibrium³²

$$\frac{[MA]_{PEC}^2}{[MA]_S^2} = e^{f\Delta H_{PEC}/RT}$$
 [6]

where salt is forced into the PEC to balance the entropy of salt in solution. For a ΔH_{PEC} = 0 salt/PE combination, [MA]_{PEC} = [MA]_s, experimentally demonstrated for the PDADMA/PSS system doped with KBr.³²

Establishing the level of doping requires measuring ion concentrations within PECs as a function of added salt. This can be done with a range of analytical methods, but the optimum technique, in our experience, uses radiolabeled ions. ⁴⁵ In the present work, a series of sodium salts containing the $^{22}\text{Na}^+$ label provided rapid, unambigous and precise measurements of salt NaA content (where A- = acetate, Ac-, Cl-, Br-, I-, or ClO₄-). The sample was simply soaked in a solution of NaA containing sufficient $^{22}\text{Na}^+$ to yield a count rate of at least 100 per second (100 cps) when placed on a 3 mm thick piece of plastic scintillator. When a series of measurements on a sample was finished, the sample was rinsed in water, weighed, dried and reweighed to obtain accurate water and dry polymer mass.

The main source of error in this measurement is from counting statistics. The absolute error is (total counts)^{1/2}, which means the relative error is 1% for 10^4 counts, 0.3% for 10^5 counts and so on. Low-activity samples (e.g. 100 cps) were counted for a few minutes so the counting error (precision) was better than \pm 1%. The accuracy was also good (estimated to be \pm 5%) demonstrated by close agreement of the duplicate samples in Supporting Information Figure S2.

Doping Equilibration Time

Although all the ions used were previously found⁴⁶ to have similar PEC diffusion coefficients ($5-10\times10^{-7}~{\rm cm^2~s^{-1}}$ at room temp), it was discovered that the time for the doping level to stabilize depended on the counterion. After a step change in solution NaA concentration, hydrophobic ions I- and ${\rm ClO_4^{-1}}$ took hours to weeks to stabilize (Figure 1), whereas salt diffusion through these 1 mm thick samples should have been complete within about 3 h. This surprising result correlates with high amounts of swelling in these ions, suggesting substantial chain rearrangement, possibly to accommodate "nanopools" of co-ions, occurs during re-equilibration.

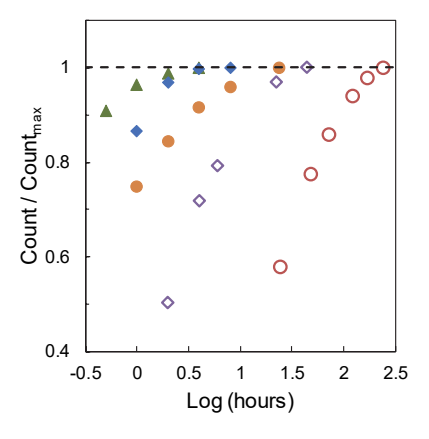


Figure 1. Time needed to reach doping equilibrium for PSS/PDADMA disks after a step change in salt NaA concentration. NaA = NaAc, ▲; NaCl, ♦; NaBr, ♠; NaI, ♦; and NaClO₄, ∘. For NaAc: from 0.1 to 0.9 m; NaCl and NaBr: from 0.2 to 0.3 m; NaI and NaClO₄: from 0.25 to 0.3 m. Counts are normalized to those at the longest time point. It is clear that NaI and NaClO₄ have not reached a steady state, or equilibrium, doping level.

Equilibrium Doping

Measurements of ion content and sample volume, approaching equilibrium, *versus* solution content are shown in Figure 2.

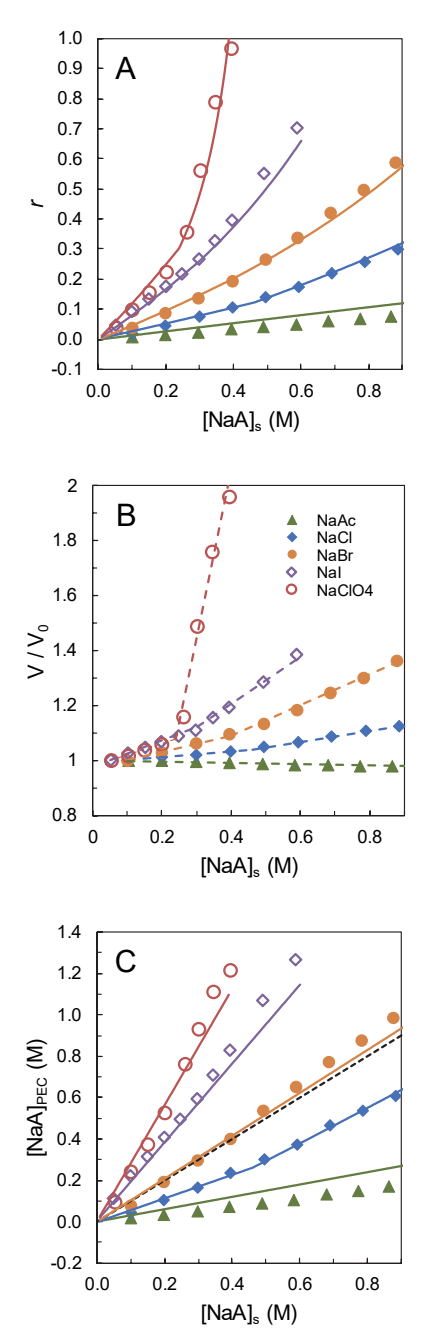


Figure 2. A, [NaA]_{PEC}/[PE]_{PEC} mole ratio, r, vs. solution salt concentration, [NaA]_s. Solid lines are obtained using Equation 2 and the fits in Panel C of this Figure. The inflection point for NaAc occurs at higher [NaAc]_s, about 2 M, shown in Supporting Information Figure S3; **B**, sample volume vs. [NaA]_s, normalized to beginning volume, dotted lines are a guide to the eye; **C**, salt concentration in PEC, [NaA]_{PEC} vs. [NaA]_s. NaA = NaAc, \blacktriangle ; NaCl, \spadesuit ; NaBr, \blacksquare ; NaI, \lozenge ; and NaClO₄, \circ . Each data point for NaI was allowed 24 h

to reach steady state. The equilibration time for each NaClO₄ concentration was 3 days up to r = 0.2, and 2 weeks for each point thereafter. Solid lines are from Equations 7 and 8 using the parameters in Table 3. Temperature = 25 °C.

A particularly interesting feature of the doping curves in Figure 2 is seen: at some point along the $[NaA]_s$ axis (Figure 2A) there is an upwards kink in the doping level. This change in $dr/d[NaA]_s$ is more clearly seen in Supporting Information Figure S3, showing individual plots of r versus $[NaA]_s$ The transition in slope occurs at the same point as a change in the volume slope (Figure 2B) which is mainly caused by an increase in the water content (Supporting Information Figure S4). The total ion concentration (Figure 2C), governed by the equilibrium between PEC ions and solution ions in Equation 6, increases but shows no transition in slope.

The inflection point change in doping and volume shown in Figure 2, not previously reported, is only unambiguously observable because of the high precision of the radiolabel doping method. It is interpreted to coincide with the transition between a glassy state and a rubbery state. The r value at the transition, labeled r_{tr} , was measured from the intercept of the two slopes seen in the expanded plots of Figure 2A in Supporting Information Figure S3. Before r_{tr} , there is limited volume for hydrated ions and they must break Pol⁺Pol⁻ pairs as counterions to access the PEC. (Route 1 in Scheme 1). After the transition, NaA can enter as either counterions or co-ions. The classical idea of polymer free volume, Scheme 1, may be compared with the "ion-accessible volume" concept described here (Figure 2): volume is accessible to co-ions after r_{tr} (a doping level of about 0.2).

Table 1 summarizes the features of the doping transition at $[NaA]_s = [NaA]_{s,tr}$. A few general trends are seen. The range of r_{tr} values is from 0.12 to 0.28. r_{tr} increases with the hydrophobicity of the ion (except for acetate) and occurs at a volume fraction of water plus ion of 0.44 \pm 0.03.

Table 1. r_{tr} , [NaA]_{tr}, volume fraction of ion, water and (ion + water) values at inflection points in Figure 2.

	r _{tr}	[NaA] _{tr} ,	ϕ_{ion}	φ water	$oldsymbol{\phi}_{polymer}$	$oldsymbol{\phi}$ water+ion	
	·u	М	PIOII	y water	± 0.005	±0.005	
NaAc	0.17	1.83	0.021	0.402	0.58	0.423	
NaCl	0.12	0.46	0.007	0.445	0.55	0.452	
NaBr	0.19	0.40	0.013	0.469	0.52	0.482	
Nal	0.26	0.30	0.024	0.421	0.55	0.445	
NaClO ₄	0.28	0.24	0.031	0.403	0.57	0.434	

lons usually enter the PEC with plenty of water. Acetate is the only ion of which we are aware to cause *dehydration* on doping. This effect is illustrated in Figure 3, which shows the number of water molecules normalized to PE. Table 2 details the net number of water molecules per NaA introduced into the PEC on doping for r < 0.2. A break is observed after $r_{\rm tr}$, consistent with additional water per NaA (see Supporting Information S4) after this point.

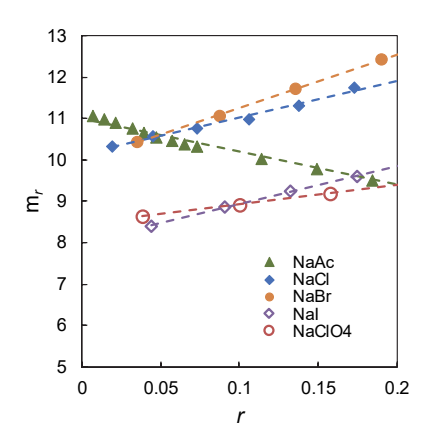


Figure 3. Number of water molecules per PE, m_r , *versus* [NaA]_{PEC}/[PE]_{PEC} ratio, r. NaA = NaAc, \blacktriangle ; NaCl, \blacklozenge ; NaBr, \blacksquare ; NaI, \diamondsuit ; and NaClO₄, \circ .

Table 2. Net water molecules per NaA doped into PEC, H_2O/NaA ; and extrapolated number of water molecules per Pol⁺Pol⁻ as NaA \rightarrow 0, m_{r0} , from Figure 3 (fitting with only r < 0.2 data).

	H₂O/NaA	m _{r0}
Ac-	-8.6	11.0
Cl ⁻	8.8	10.1
Br	12.8	10.0
 -	9.2	8.0
CIO ₄ -	4.5	8.5

The exceptional behavior of acetate is interpreted to be a result of exceedingly weak doping, requiring a high solution concentration NaAc, which exerts a high osmotic pressure and extracts more water than the salt brings in at a particular [NaAc]_s.

Counter- versus Co-ions, Correlation with Enthalpy Changes.

Isothermal calorimetry, ITC, provided the enthalpy of complexation when Pol⁺A- and Pol⁻M⁺, both in solutions of salt MA, were mixed.^{39, 47, 48, 49, 50, 51, 52, 53, 54, 55, 56} As [NaA]_s increased the resulting PEC ended up at a higher r (Figure 2A). Reliable ITC over a range of r was only possible in NaA = NaCl, since ITC in NaBr was virtually athermal, PDADMA(I) was insoluble, PDADMA(ClO₄) was insoluble, and NaAc is a very poor doping agent (Figure 2A).

ITC of the PEC formation by PDADMA(CI) and PSSNa in NaCI (an example of the raw thermogram is given in Supporting Information Figure S5) revealed two distinct enthalpy regimes. At [NaCI] < 0.5 M the complexation provided much more enthalpy change (Figure 4). For [NaCI] > 0.5 M the enthalpy change was still exothermic, but low and remained so.

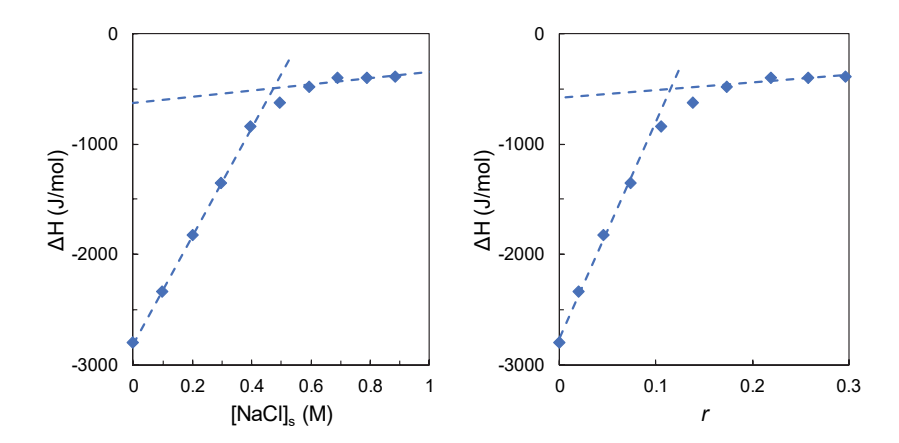


Figure 4. Isothermal titration of 10 mM PSSNa into 0.5 mM PDADMA(CI) at 25 °C in the presence of increasing [NaCI] (left). The concentration axis is transformed into r using Figure 2A (right). The change in slope corresponds to the change in doping behavior in Figure 2A seen at $r_{\rm tr} = 0.12$.

[MA]_s = 0 yields fully paired PEC that has no salt content (as is commonly found^{1, 2}). ΔH extrapolated to [MA] = 0 is termed ΔH_{PEC} . The enthalpy changes in Figure 4 mirror the changes in slopes shown in Figure 2. The break points, at about 0.5 M, are interpreted to signal a change between counter- and co-ions roles for NaCl along with a change in ΔH for these two roles: for $r < r_{tr}$, ions enter the PEC with fraction f_b as counterions (Scheme 2, Path 1 shows f_b = 1) and the enthalpy for this path is $f_b\Delta H_{PEC}$. For $r > r_{tr}$, additional doping yields a mix of co-ions (Scheme 2, Paths 2) with fraction f_a counterions. Equation 6 is rearranged as follows

$$[MA]_{PEC} = [MA]_{S} e^{f_{av}\Delta H_{PEC}/2RT}$$
 [7]

where f_{av} is the average for the entire doping to that particular [MA]_s, determined as follows: before r_{tr} , $f_{av} = f_b$

after r_{tr} , which occurs at [MA]_{s,tr},

$$f_{av} = f_b \frac{[MA]_{s,tr}}{[MA]_s} + f_a \frac{[MA]_s - [MA]_{s,tr}}{[MA]_s}$$
[8]

A comparison of ΔH intercepts (-2800 versus -580 J mol⁻¹) in Figure 4 suggests only 21% (i.e. f_a = 0.21 or 580/2800) of NaCl entering the PEC breaks Pol⁺Pol⁻ pairs after $r_{\rm fr}$.

Figure 2C shows good agreement of fits to experimental data for [NaA]_{PEC} versus [NaAc]_s, [NaCl]_s and [NaBr]_s using Equations 7 and 8 and the Δ H, f_a , and f_b values in Table 3. Since PDADMA(I) and PDADMA(ClO₄) were insoluble, ITC of their complexation with PSSNa could not be performed and Δ H_{PEC} for NaClO₄ and Nal were estimated by adding PDADMA(Cl) to Nal or NaClO₄ (see Supporting Information Figure S5 for raw ITC data).

Table 3. Enthalpies ΔH_{PEC} of PDADMA(A) and PSSNa complexation along with fraction counterions before, f_b , and fraction after, f_a , the transition in various salt solutions NaA.

Salt NaA	ΔH _{PEC} (J mol ⁻ ¹)	f_b	f _a	
NaAc	-6027a	1	0.2	
NaCl	-2800	1	0.21 ^b	
NaBr	189ª	1	1°	
Nal	3200 ^d	1	1	
NaClO ₄	12800 ^d	0.4	0.4	

^afrom reference ³²

In Table 3, f_b has been fixed at 1, consistent with the idea that all ions are counterions before the transition. The only exception is for NaClO₄, where f_b = 1 would have strongly overestimated [NaClO₄]_{PEC} in Figure 2C. Instead, a best fit value of 0.4 suggests 40% of ions are counterions before and after the transition. The reason for this is at least partly due to the fact that [ClO₄]_{PEC} has not yet reached equilibrium, as indicated by Figure 1. The NaCl fit in 2A, magnified in Supporting Information Figure S3, is excellent using f_b = 1 and f_a = 0.21 from calorimetry.

Note that an endothermic ΔH_{PEC} indicates a *preference* of at least one of the counterions for Pol⁺ or Pol⁻, also termed a "specific interaction." In the present case, I⁻ and CIO₄⁻ both precipitate PDADMA(CI), a strong specific interaction of I⁻ and CIO₄⁻ with DADMA⁺ relative to CI⁻. With an interaction enthalpy of -3.2 kJ mol⁻¹ and -12.8 kJ mol⁻¹ (relative to sulfonate, SS⁻) for these respective ions, the fraction of counterions should remain close to 1 for salts with these anions over all [NaA]. Conversely, an exothermic ΔH_{PEC} indicates an anti-preference of DADMA⁺ for CI⁻ (relative to SS⁻). In this case, most ions are expected to remain co-ions after r_{tr} which explains why NaCl is able to swell, but not dissolve, PDADMA/PSS, even at concentrations approaching 5 M.³⁶

Assigning most of the enthalpy changes to the intrinsic →extrinsic conversion shown in Equation 4 assumes co-ions are in an environment similar to that found in aqueous solution and do not contribute substantially to ΔH_{PEC}.^{32, 52} Relatively recently, it has been shown that the range of water structure disruption by charges in an aqueous environment, which contains information regarding specific interactions between charges, extends only to the first solvation shell.^{57, 58} This would support the assumption that only ions in counterion "parking spots" next to the polymer repeat unit show differences in specific interactions with polyelectrolyte (distance between charges, distribution and polarizability of ions) which lead to a change in the water structure around the polyelectrolyte, and an enthalpy change.³⁹

Discerning between counter- and co-ion population based on location offers considerable experimental challenges – the position of these differs by a nm or so and the populations are likely rapidly exchanging places. Using $\Delta H_{\text{PEC}},$ if it can be measured reliably, to signal this subtle yet important distinction appears to be the only

bfrom ITC

[°]because ΔH_{PEC} is so small f_a and f_b are not fit with accuracy

dmeasured by adding PDADMA(CI) to NaI or NaClO4

report, though indirect, available for the degree of Pol⁺Pol⁻ breaking/pairing. Fortunately, ITC measurements of complexation are relatively straightforward.

Pair Breaking Versus Water in Plasticization

The precise relationship between doping and ion concentration in Figure 2 was used in an attempt to shed light on the relative roles of water and ions in plasticizing PECs. On one hand, ions usually introduce more water into PECs, and water is known to be an efficient plasticizer in general and for PECs in particular.^{2, 3, 10, 59, 60, 61} At the same time, ions break crosslinks, making the material softer. Which of these has more influence on the mechanical properties of PECs?

Figure 5 compares viscoelastic properties *versus* temperature of the same PEC doped with different NaA to r = 0.20. A drop in storage and loss modulus, G' and G", at the glass transition occurs for all NaA. Temperatures were scanned up and down to verify no irreversible changes in the material had occurred (e.g. values of G' and G" are the same at the starting temperature in Figure 5). Tan δ provides reproducible T_g values which are tabulated in Table 4.

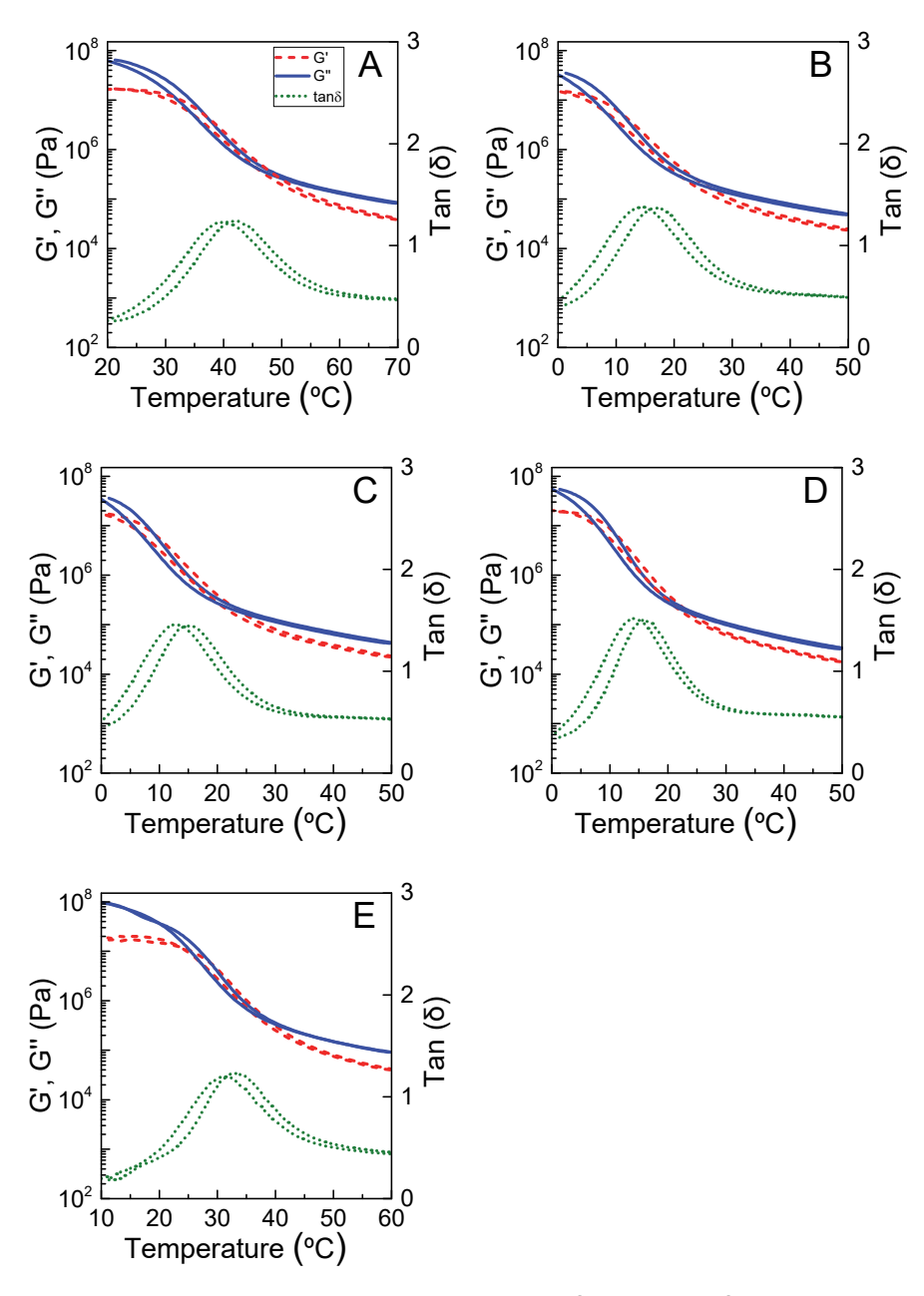


Figure 5. Viscoelastic measurements at a frequency of 0.1 Hz while ramping the temperature at 1 °C min⁻¹ for PSS/PDADMA disk in NaA solutions of the appropriate concentration to dope to r = 0.2 (see Table 4). Panel A, NaAc; B, NaCl; C, NaBr; D, NaI; and E, NaClO₄. Both heating and cooling ramps are shown. Small differences in G', solid line, G" dashed line, and tan δ , dotted line, between heating and cooling are from the thermal lag in the sample cell. T_g was taken as the midpoint between cooling and heating tan δ peaks.

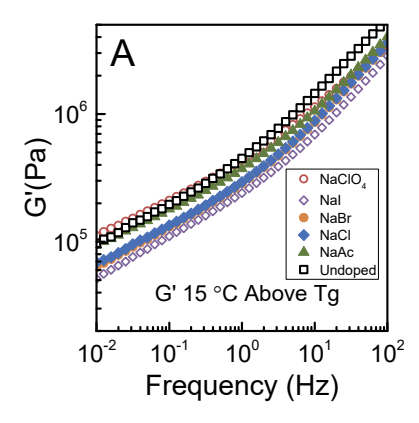
Table 4. T_g of PSS/PDADMA sample in r = 0.2 NaA solutions determined with viscoelastic measurements (dynamic mechanical analysis) at 0.1 Hz, along with volume fractions of water and ions at r = 0.2.

Salt Type	M at r = 0.2	$oldsymbol{\phi}_{ ext{water}}$	Ф ions	Ø (water+ions)	Water per intrinsic site	T _g (°C)
NaAc	2.046	0.394	0.026	0.420	11.6	41.0
NaCl	0.648	0.461	0.011	0.472	14.9	15.7
NaBr	0.416	0.472	0.014	0.486	15.7	14.2
Nal	0.226	0.410	0.019	0.429	12.3	14.9
NaClO ₄	0.180	0.398	0.025	0.423	11.7	31.7
Undoped	-	0.393	0	0.393	9	39.6

Conclusions regarding the relative importance of water versus doping on T_g are not definitive: because T_g clearly varies for different ions at the same doping level, the degree of pair breaking is not the major factor. But the water content, normalized to the number of intrinsic sites (80% of the total sites), as suggested by Zhang et al. 10 , also does not fully predict the ordering of T_g , although broadly speaking the two doped PECs with the least water (NaAc and NaClO4) have the highest T_g . The contributions of water and pair breaking to moderating the glass transition appear to be a complex interplay between the location of hydration water and how different polymer-counterion pairs might relax. Molecular dynamics simulations of PDADMA/PSS PEC by Zhang et al. 60 support this more complex picture.

Assuming free volume is added by both water and ions, Table 4 shows a change between room temperature glassy and rubbery materials at a $\phi_{\text{(water+ion)}}$ of 0.43 (see Supporting Information Figure S6 for a clear illustration), in reasonable consistency with Table 1, which shows r_{tr} to be at a $\phi_{(water+ion)}$ of about 0.44. However, the ordering of T_q in Table 4 does not follow the ordering of r_{tr} in Table 1 indicating the ion-accessible volume change experienced by ions and their disposition is not in perfect registry with polymer free volume changes around the glass transition. A comparison of $\phi_{\text{(water+ion)}}$, around 40%, with the polymer free volume at T_g, presumed to be about 2.5%, 62 illustrates the difficulty in assigning whatever contribution $\phi_{\text{(water+ion)}}$ makes to the polymer free volume, especially if some ions hold water more tenaciously than others. Another challenge is reconciling the kinetic nature of the glass transition with the (presumed) equilibrium nature of doping. Tg decreases if the material is probed more slowly, for example at lower heating rates or at lower deformation frequencies. Yet Tg is not influenced by the doping rate as long as a particular equilibrium composition has been attained. The influence of doping on T_g is best compared with plasticizers:26 the T_g does not depend on the rate the plasticizer is added, but on the composition. In a similar way, the total volume of plasticizer added is greater than the (more conceptual) "free" volume added to the polymer.

The influence of doping on dynamics above T_g was compared by performing time-temperature superposition of the five doped samples by comparing them at 15 °C above their T_g s (individual data in Supporting Information Figure S7). Although responses were brought close, complete superposition was not achieved (see Figure 6). G' and G" for r = 0.2 were generally lower than for the undoped PEC. Interestingly, perchlorate had the highest G' and G" of all the doped PECs in Figure 6, consistent with the possibility in Table 3 that the fraction of Pol+Pol- pairs broken by added NaA is significantly less than 1 at r = 0.2.



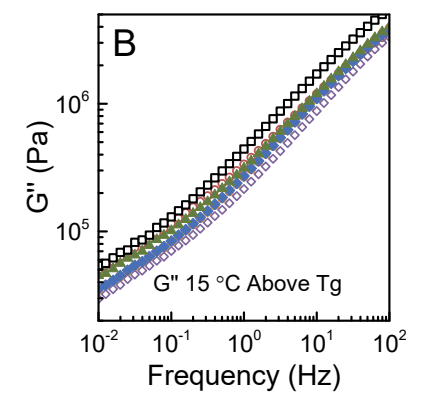


Figure 6. Linear viscoelasticity, under a frequency sweep, showing G', **A**, and G", **B**, for PEC in r = 0.2 NaA solutions at 15 °C above T_g. NaA = NaAc, **△**; NaCl, **♦**; NaBr, **•**; NaI, \Diamond ; NaClO₄, \circ ; and undoped, \Box Data points for NaBr and NaCl superimpose.

Are my PECs glassy?

With an increasingly greater variety of complexes/coacervates reported, this is a good question. Because a main variable is the water content, information on the environment of the PEC is needed – is it in ambient or is it immersed in aqueous solutions? Most PECs in multilayer or bulk form are either fully immersed in aqueous, or operate at some undefined ambient relative humidity, although both should provide an equilibrium value for water content. From our experience, PECs immersed in aqueous solutions have T_g around room temperature if they have a volume fraction water of about 50%. Liquid-like PECs with higher water content are traditionally labeled "coacervates," whereas solid-like PECs are usually termed "complexes." But it is possible to turn a liquid-like PEC into a glassy material by simply removing some of the water.

When determining the hydration level of PECs it is important to account for porosity. Porosity on a scale larger than molecular (i.e. > a few nm) is not expected to influence T_g. Larger pores (or internal microphase separation), are ubiquitous features of PECs, solid (or liquid). They result from either the method of PEC formation⁶³ or from an adjustment in the equilibrium composition of PEC components in response to a change in salt concentration, pH, or temperature.^{64, 65, 66, 67} For example, going from a high salt to a low salt environment, small ions and water are quickly lost from PEC, but the more glassy the material, the slower the polymer rearranges, and instead of

being expelled to bulk solution, the water is expelled internally into pores: a microphase separation.^{28, 68, 69} These pores cause light to be scattered, unless the PEC is index matched, e.g. in solutions of high [MA], leading to a white appearance of the PEC. Liquidlike PECs also experience microphase separation but given time, and encouraged by "annealing" at a modestly higher temperature, the microphases fuse into a continuous, optically clear, PEC phase and dilute solution phase.

Conclusions

A change in salt doping behavior of a PEC known to have a T_g near room temperature was interpreted to coincide with the appearance of additional polymer free volume. Salt entering the PEC is believed to adopt the role of either counterion or coion. An initial stronger enthalpic stage of doping, representing 15 to 20 mole% of the total number of paired polyelectrolyte repeat units, supported this interpretation. Because PECs are amorphous, it is a challenge to measure the relative locations of ions and repeat units directly, although there may be NMR techniques suited for the job, as they are for elucidating "structure" in amorphous regions of folded protein.⁷⁰

Theory and simulation, such as molecular dynamics, may provide insight on the precise disposition of ions relative to repeat units. It is recommended that a site-specific model be adopted, as opposed to one based on continuum electrostatics. This model would place ions randomly within the PEC to balance the external entropy of solution ions (Donnan equilibrium). The free (non-polymer) volume would be divided into the volume within one ion diameter of the polymer chain, subject to "specific" interactions, and the balance of the free volume would be equally available to all ions as long as they are separated from each other by at least one solvent molecule. Hydration of ions would dictate whether they are strongly associated with Pol⁺ or Pol⁻: weak hydration would be more likely to yield exothermic contact Pol⁺A⁻ pairing, whereas stronger ion hydration should give solvent separated pairs in the resulting in less favorable enthalpy changes.

For undoped and doped PEC, the role of water in controlling T_g appears to be one of a traditional plasticizer - mainly to add free volume. Regarding viscoelastic properties above T_g , added water decreases the volume fraction of polymer chains and accelerates relaxation dynamics at all levels. Doping also accelerates viscoelastic relaxations of polymer chains by decreasing the number of "sticky" Pol+Pol- pairs.

Many of the PECs used currently and historically are fluid-like coacervates – already above T_g – where there is an unknown mix of counter and co-ions. For stoichiometric PECs, there are two points in the salt/composition phase diagram where the fraction of paired Pol+Pol- is known: if the PEC is salt-free, all Pol+ and Pol- have "found" each other and y = 0. At the point, if it exists, where a liquid-liquid phase separated coacervate turns into a clear, single phase, the fraction of Pol+Pol- must approach zero, i.e. $y \rightarrow 1$ (although there may still be a small number of pairs yielding clusters of polyelectrolyte). Between these two extremes remains a fertile ground for exploring the role of counterions with as much attention to their specific locations as possible.

Supporting Information

Radiolabel calibration curves for all salts; comparison of the doping of two samples; magnified plots of r versus [NaA]s to show transition; wt% water versus [NaA]s; ITC calorimetry data; correlation of T_g with volume fraction of water + ions; individual viscoelastic measurements of NaA-doped PECs at $T = T_g + 15\,^{\circ}\text{C}$.

17

Author Information Corresponding Author *Email: jschlenoff@fsu.edu

Notes

The authors declare no competing financial interest

Acknowledgments

This work was supported by a grant from the National Science Foundation (DMR-1809304).

References

- 1. Michaels, A. S.; Miekka, R. G. Polycation-Polyanion Complexes: Preparation and Properties of Poly(Vinylbenzyltrimethylammonium Styrenesulfonate). *Journal of Physical Chemistry* **1961**, *65*, 1765-73.
- 2. Michaels, A. S. Polyelectrolyte Complexes. *Journal of Industrial and Engineering Chemistry* **1965**, *57*, 32-40.
- 3. Bixler, H. J.; Michaels, A. S. Polyelectrolyte Complexes. In *Encyclopedia of Polymer Science and Technology*; Interscience: New York, 1969; Vol. 10, pp 765-80.
- 4. Sing, C. E.; Perry, S. L. Recent Progress in the Science of Complex Coacervation. *Soft Matter* **2020**, *16*, 2885-2914.
- 5. Tsuchida, E.; Osada, Y.; Ohno, H. Formation of Interpolymer Complexes. *J Macromol Sci Phys* **1980**, *B17*, 683-714.
- 6. Bungenberg de Jong, H. G.; Kruyt, H. R. Coacervation (Partial Miscibility in Colloid Systems). *Proc. Sect. Sci. K. Ned. Akad. Wetenschappen* **1929**, *32*, 849-856.
- 7. Fuoss, R. M.; Sadek, H. Mutual Interaction of Polyelectrolytes. *Science* **1949**, *110*, 552-4.
- 8. Wang, Q. F.; Schlenoff, J. B. The Polyelectrolyte Complex/Coacervate Continuum. *Macromolecules* **2014**, *47*, 3108-3116.
- 9. Huglin, M. B.; Webster, L.; Robb, I. D. Complex Formation between Poly(4-Vinylpyridinium Chloride) and Poly[Sodium(2-Acrylamido-2-Methyl Propane Sulfonate)] in Dilute Aqueous Solution. *Polymer* **1996**, *37*, 1211-1215.
- 10. Zhang, Y.; Batys, P.; O'Neal, J. T.; Li, F.; Sammalkorpi, M.; Lutkenhaus, J. L. Molecular Origin of the Glass Transition in Polyelectrolyte Assemblies. *ACS Central Science* **2018**, *4*, 638-644.
- 11. Lyu, X.; Clark, B.; Peterson, A. M. Thermal Transitions in and Structures of Dried Polyelectrolytes and Polyelectrolyte Complexes. *Journal of Polymer Science Part B: Polymer Physics* **2017**, *55*, 684-691.
- 12. Fu, J.; Fares, H. M.; Schlenoff, J. B. Ion-Pairing Strength in Polyelectrolyte Complexes. *Macromolecules* **2017**, *50*, 1066-1074.
- 13. Köhler, K.; Shchukin, D. G.; Möhwald, H.; Sukhorukov, G. B. Thermal Behavior of Polyelectrolyte Multilayer Microcapsules. 1. The Effect of Odd and Even Layer Number. *Journal of Physical Chemistry B* **2005**, *109*, 18250-18259.
- 14. Köhler, K.; Möhwald, H.; Sukhorukov, G. B. Thermal Behavior of Polyelectrolyte Multilayer Microcapsules: 2. Insight into Molecular Mechanisms for the PDADMAC/PSS System. *Journal of Physical Chemistry B* **2006**, *110*, 24002-24010.
- 15. Shamoun, R. F.; Hariri, H. H.; Ghostine, R. A.; Schlenoff, J. B. Thermal Transformations in Extruded Saloplastic Polyelectrolyte Complexes. *Macromolecules* **2012**, *45*, 9759-9767.
- 16. Sung, C.; Hearn, K.; Lutkenhaus, J. Thermal Transitions in Hydrated Layer-by-Layer Assemblies Observed Using Electrochemical Impedance Spectroscopy. *Soft Matter* **2014**, *10*, 6467-6476.
- 17. Yang, M.; Shi, J.; Schlenoff, J. B. Control of Dynamics in Polyelectrolyte Complexes by Temperature and Salt. *Macromolecules* **2019**, *52*, 1930-1941.
- 18. Schaaf, P.; Schlenoff, J. B. Saloplastics: Processing Compact Polyelectrolyte Complexes. *Advanced Materials* **2015**, *27*, 2420-2432.
- 19. Shamoun, R. F.; Reisch, A.; Schlenoff, J. B. Extruded Saloplastic Polyelectrolyte

- Complexes. Advanced Functional Materials 2012, 22, 1923-1931.
- 20. Gai, M.; Frueh, J.; Kudryavtseva, V. L.; Mao, R.; Kiryukhin, M. V.; Sukhorukov, G. B. Patterned Microstructure Fabrication: Polyelectrolyte Complexes vs Polyelectrolyte Multilayers. *Scientific Reports* **2016**, *6*, 37000.
- 21. Gao, C.; Wang, B.; Feng, J.; Shen, J. Irreversible Compression of Polyelectrolyte Multilayers. *Macromolecules* **2004**, *37*, 8836-8839.
- 22. Kelly, K. D.; Schlenoff, J. B. Spin-Coated Polyelectrolyte Coacervate Films. *ACS Applied Materials & Interfaces* **2015**, *7*, 13980-13986.
- 23. Haile, M.; Sarwar, O.; Henderson, R.; Smith, R.; Grunlan, J. C. Polyelectrolyte Coacervates Deposited as High Gas Barrier Thin Films. *Macromolecular Rapid Communications* **2017**, *38*, 1600594.
- 24. Duan, Y.; Wang, C.; Zhao, M.; Vogt, B. D.; Zacharia, N. S. Mechanical Properties of Bulk Graphene Oxide/Poly(Acrylic Acid)/Poly(Ethylenimine) Ternary Polyelectrolyte Complex. *Soft Matter* **2018**, *14*, 4396-4403.
- 25. Huglin, M. B.; Rego, J. M. Study of Polymer Blends Based on Poly(Vinylpyridines) and Acidic Polymers. *Polymer* **1990**, *31*, 1269-1276.
- 26. Wypych, G. *Handbook of Plasticizers*; ChemTee Publishing ; William Andrew Inc.: Norwich, NY, 2004. p 687 pages.
- 27. Yang, Y.-H.; Haile, M.; Park, Y. T.; Malek, F. A.; Grunlan, J. C. Super Gas Barrier of All-Polymer Multilayer Thin Films. *Macromolecules* **2011**, *44*, 1450-1459.
- 28. Fares, H. M.; Wang, Q.; Yang, M.; Schlenoff, J. B. Swelling and Inflation in Polyelectrolyte Complexes. *Macromolecules* **2019**, *52*, 610-619.
- 29. Strobl, G. *The Physics of Polymers, 3rd Ed*; Springer: Berlin, 2010.
- 30. Hempel, E.; Hempel, G.; Hensel, A.; Schick, C.; Donth, E. Characteristic Length of Dynamic Glass Transition near Tg for a Wide Assortment of Glass-Forming Substances. *Journal of Physical Chemistry B* **2000**, *104*, 2460-2466.
- 31. Berthier, L.; Biroli, G.; Bouchaud, J.-P.; Cipelletti, L.; Masri, D. E.; L'Hôte, D.; Ladieu, F.; Pierno, M. Direct Experimental Evidence of a Growing Length Scale Accompanying the Glass Transition. *Science* **2005**, *310*, 1797-1800.
- 32. Schlenoff, J. B.; Yang, M.; Digby, Z. A.; Wang, Q. Ion Content of Polyelectrolyte Complex Coacervates and the Donnan Equilibrium. *Macromolecules* **2019**, *52*, 9149-9159.
- 33. Krebs, T.; Tan, H. L.; Andersson, G.; Morgner, H.; Gregory Van Patten, P. Increased Layer Interdiffusion in Polyelectrolyte Films Upon Annealing in Water and Aqueous Salt Solutions. *Physical Chemistry Chemical Physics* **2006**, *8*, 5462-5468.
- 34. Spruijt, E.; Sprakel, J.; Lemmers, M.; Stuart, M. A. C.; van der Gucht, J. Relaxation Dynamics at Different Time Scales in Electrostatic Complexes: Time-Salt Superposition. *Physical Review Letters* **2010**, *105*, 208301.
- 35. Liu, Y.; Momani, B.; Winter, H. H.; Perry, S. L. Rheological Characterization of Liquid-to-Solid Transitions in Bulk Polyelectrolyte Complexes. *Soft Matter* **2017**, *13*, 7332-7340.
- 36. Ali, S.; Prabhu, V. Relaxation Behavior by Time-Salt and Time-Temperature Superpositions of Polyelectrolyte Complexes from Coacervate to Precipitate. *Gels* **2018**, *4*, 11.
- 37. Marciel, A. B.; Srivastava, S.; Tirrell, M. V. Structure and Rheology of Polyelectrolyte Complex Coacervates. *Soft Matter* **2018**, *14*, 2454-2464.
- 38. Philipse, A.; Vrij, A. The Donnan Equilibrium: I. On the Thermodynamic Foundation of the Donnan Equation of State. *Journal of Physics: Condensed Matter* **2011**, *23*, 194106.
- 39. Fu, J. C.; Schlenoff, J. B. Driving Forces for Oppositely Charged Polyion Association in Aqueous Solutions: Enthalpic, Entropic, but Not Electrostatic. *Journal of the American Chemical Society* **2016**, *138*, 980-990.
- 40. Hofmeister, F. *Arch. Exp. Pathol. Pharmakol.* **1888,** *24*, 247-260.
- 41. Z. Moghaddam, S.; Thormann, E. The Hofmeister Series: Specific Ion Effects in Aqueous Polymer Solutions. *Journal of Colloid and Interface Science* **2019**, *555*, 615-635.

- 42. Matsuno, R.; Kokubo, Y.; Kumagai, S.; Takamatsu, S.; Hashimoto, K.; Takahara, A. Molecular Design and Characterization of Ionic Monomers with Varying Ion Pair Interaction Energies. *Macromolecules* **2020**, *53*, 1629-1637.
- 43. Trinh, C. K.; Schnabel, W. Ionic-Strength Dependence of the Stability of Polyelectrolyte Complexes Its Importance for the Isolation of Multiply-Charged Polymers. *Angew Makromol Chem* **1993**, *212*, 167-179.
- 44. Bungenberger de Jong, H. G. In *Colloid Science*, Kruyt, H. R., Ed.; Elsevier: Amsterdam, 1949; Vol. 2.
- 45. Fares, H. M.; Schlenoff, J. B. Equilibrium Overcompensation in Polyelectrolyte Complexes. *Macromolecules* **2017**, *50*, 3969-3979.
- 46. Ghostine, R. A.; Shamoun, R. F.; Schlenoff, J. B. Doping and Diffusion in an Extruded Saloplastic Polyelectrolyte Complex. *Macromolecules* **2013**, *46*, 4089-4094.
- 47. Laugel, N.; Betscha, C.; Winterhalter, M.; Voegel, J. C.; Schaaf, P.; Ball, V. Relationship between the Growth Regime of Polyelectrolyte Multilayers and the Polyanion/Polycation Complexation Enthalpy. *Journal of Physical Chemistry B* **2006**, *110*, 19443-19449.
- 48. Feng, X.; Leduc, M.; Pelton, R. Polyelectrolyte Complex Characterization with Isothermal Titration Calorimetry and Colloid Titration. *Colloid Surface A* **2008**, *317*, 535-542.
- 49. Priftis, D.; Laugel, N.; Tirrell, M. Thermodynamic Characterization of Polypeptide Complex Coacervation. *Langmuir* **2012**, *28*, 15947-15957.
- 50. Alonso, T.; Irigoyen, J.; Iturri, J. J.; Larena, I. L.; Moya, S. E. Study of the Multilayer Assembly and Complex Formation of Poly(Diallyldimethylammonium Chloride) (PDADMAC) and Poly(Acrylic Acid) (PAA) as a Function of Ph. *Soft Matter* **2013**, *9*, 1920-1928.
- 51. Priftis, D.; Megley, K.; Laugel, N.; Tirrell, M. Complex Coacervation of Poly(Ethylene-Imine)/Polypeptide Aqueous Solutions: Thermodynamic and Rheological Characterization. *J. Coll. Interfac. Sci.* **2013**, *398*, 39-50.
- 52. Požar, J.; Kovačević, D. Complexation between Polyallylammonium Cations and Polystyrenesulfonate Anions: The Effect of Ionic Strength and the Electrolyte Type. *Soft Matter* **2014**, *10*, 6530-6545.
- 53. Vitorazi, L.; Ould-Moussa, N.; Sekar, S.; Fresnais, J.; Loh, W.; Chapel, J. P.; Berret, J. F. Evidence of a Two-Step Process and Pathway Dependency in the Thermodynamics of Poly(Diallyldimethylammonium Chloride)/Poly(Sodium Acrylate) Complexation. *Soft Matter* **2014**, *10*, 9496-9505.
- 54. Kremer, T.; Kovačević, D.; Salopek, J.; Požar, J. Conditions Leading to Polyelectrolyte Complex Overcharging in Solution: Complexation of Poly(Acrylate) Anion with Poly(Allylammonium) Cation. *Macromolecules* **2016**, *49*, 8672-8685.
- 55. Lounis, F. M.; Chamieh, J.; Leclercq, L.; Gonzalez, P.; Geneste, A.; Prelot, B.; Cottet, H. Interactions between Oppositely Charged Polyelectrolytes by Isothermal Titration Calorimetry: Effect of Ionic Strength and Charge Density. *The Journal of Physical Chemistry B* **2017**, *121*, 2684-2694.
- 56. Bucur, C. B.; Sui, Z.; Schlenoff, J. B. Ideal Mixing in Polyelectrolyte Complexes and Multilayers: Entropy Driven Assembly. *Journal of the American Chemical Society* **2006**, *128*, 13690-13691.
- 57. Omta, A. W.; Kropman, M. F.; Woutersen, S.; Bakker, H. J. Negligible Effect of lons on the Hydrogen-Bond Structure in Liquid Water. *Science* **2003**, *301*, 347-349.
- 58. Moilanen, D. E.; Wong, D.; Rosenfeld, D. E.; Fenn, E. E.; Fayer, M. D. Ion–Water Hydrogen-Bond Switching Observed with 2D IR Vibrational Echo Chemical Exchange Spectroscopy. *Proceedings of the National Academy of Sciences* **2009**, *106*, 375-380.
- 59. Hariri, H. H.; Lehaf, A. M.; Schlenoff, J. B. Mechanical Properties of Osmotically Stressed Polyelectrolyte Complexes and Multilayers: Water as a Plasticizer. *Macromolecules* **2012**, *45*, 9364-9372.
- 60. Zhang, R.; Zhang, Y.; Antila, H. S.; Lutkenhaus, J. L.; Sammalkorpi, M. Role of Salt and

Water in the Plasticization of PDAC/PSS Polyelectrolyte Assemblies. *The Journal of Physical Chemistry B* **2017**, *121*, 322-333.

- 61. Nolte, A. J.; Treat, N. D.; Cohen, R. E.; Rubner, M. F. Effect of Relative Humidity on the Young's Modulus of Polyelectrolyte Multilayer Films and Related Nonionic Polymers. *Macromolecules* **2008**, *41*, 5793-5798.
- 62. Rubinstein, M.; Colby, R. H. Polymer Physics; Oxford University Press: New York, 2003.
- 63. Porcel, C. H.; Schlenoff, J. B. Compact Polyelectrolyte Complexes: "Saloplastic" Candidates for Biomaterials. *Biomacromolecules* **2009**, *10*, 2968-2975.
- 64. Stewart, R. J.; Wang, C. S.; Shao, H. Complex Coacervates as a Foundation for Synthetic Underwater Adhesives. *Adv Colloid Interfac* **2011**, *167*, 85-93.
- 65. Karabiyik Acar, O.; Kayitmazer, A. B.; Torun Kose, G. Hyaluronic Acid/Chitosan Coacervate-Based Scaffolds. *Biomacromolecules* **2018**, *19*, 1198-1211.
- 66. Mendelsohn, J. D.; Barrett, C. J.; Chan, V. V.; Pal, A. J.; Mayes, A. M.; Rubner, M. F. Fabrication of Microporous Thin Films from Polyelectrolyte Multilayers. *Langmuir* **2000**, *16*, 5017-5023.
- 67. Cundall, R. B.; Lawton, J. B.; Murray, D.; Phillips, G. O. Polyelectrolyte Complexes, 1. The Effect of pH and Ionic Strength on the Stoichiometry of Model Polycation—Polyanion Complexes. *Die Makromolekulare Chemie* **1979**, *180*, 2913-2922.
- 68. Sadman, K.; Delgado, D. E.; Won, Y.; Wang, Q.; Gray, K. A.; Shull, K. R. Versatile and High-Throughput Polyelectrolyte Complex Membranes Via Phase Inversion. *ACS Applied Materials & Interfaces* **2019**, *11*, 16018-16026.
- 69. Baig, M. I.; Durmaz, E. N.; Willott, J. D.; de Vos, W. M. Sustainable Membrane Production through Polyelectrolyte Complexation Induced Aqueous Phase Separation. *Advanced Functional Materials* **2020**, *30*, 1907344.
- 70. Mitrea, D. M.; Chandra, B.; Ferrolino, M. C.; Gibbs, E. B.; Tolbert, M.; White, M. R.; Kriwacki, R. W. Methods for Physical Characterization of Phase-Separated Bodies and Membrane-Less Organelles. *J Mol Biol* **2018**, *430*, 4773-4805.